Earth Syst. Sci. Data Discuss., doi:10.5194/essd-2016-2, 2016
Manuscript under review for journal Earth Syst. Sci. Data
Published: 25 January 2016

Open Access Earth System Science Data Discussions

Surface Radiation during the Total Solar Eclipse over Ny-Ålesund, Svalbard, on 20 March 2015

M. Maturilli[1], C. Ritter[1]

[1]Alfred Wegener Institute, Helmholtz Centre for Polar and Marine Research, D-14473 Potsdam, Germany

Correspondence to: M. Maturilli (marion.maturilli@awi.de)

Abstract. On 20 March 2015, a total solar eclipse occurred over Ny-Ålesund (78.9° N, 11.9° E), Svalbard, in the high Arctic. It has been the first time that the surface radiation components during the totality of a solar eclipse have been measured by a Baseline Surface Radiation Network (BSRN) station. With the Ny-Ålesund long term radiation data set as background (available at http://dx.doi.org/10.1594/PANGAEA.150000), we here present the peculiarities of the radiation components and basic meteorology observed during the eclipse event. The supplementary data set contains the basic BSRN radiation and surface meteorological data in 1-minute resolution for March 2015, and is available at http://dx.doi.org/10.1594/PANGAEA.854326. The eclipse radiation data will be a useful auxiliary data set for further studies on micro-meteorological surface-atmosphere exchange processes in the Svalbard environment, and may serve as a test case for radiative transfer studies.

1 Introduction

At the high Arctic site Ny-Ålesund (78.9° N, 11.9° E) on the archipelago of Svalbard, surface radiation measurements operated by the Alfred Wegener Institute since 1992 are contributing to the Baseline Surface Radiation Network (BSRN). The measurements include the various parameters related to solar radiation: global and reflected radiation (downward and upward solar radiation SW_{down} and SW_{up}, respectively), as well as the direct and diffuse shortwave radiation (SW_{direct} and $SW_{diffuse}$, respectively). Furthermore, the upward and downward thermal radiation components LW_{up} and LW_{down} are obtained. Detailed information about the instrumental set-up and the long term radiation observations since 1992 are given in Maturilli et al. (2015).

On 20 March 2015, the rare astronomical event of a total solar eclipse occurred over Ny-Ålesund with about 2 minutes of totality, allowing for the first time the measurement of the according special radiation conditions by a BSRN station. The eclipse was No.61 in the Saros cycle 120. Solar eclipses have inspired several earlier investigations in the field of meteorology. Surface atmospheric pressure fluctuations have been observed in connection to solar eclipses caused by the cooling of the atmosphere during the eclipse shadow period (Anderson et al., 1972; Anderson and Keefer, 1975). The pressure perturbations and induced gravity waves generated by a solar eclipse have been studied for several eclipse events (e.g. Schödel et al., 1973; Goodwin and Hobson, 1978; Seykora et al., 1985; Marty et al., 2013). Gravity wave forcing by a

Earth Syst. Sci. Data Discuss., doi:10.5194/essd-2016-2, 2016
Manuscript under review for journal Earth Syst. Sci. Data
Published: 25 January 2016

Open Access Earth System Science Data Discussions

solar eclipse has also been found in the middle atmosphere related to ozone photochemistry (Fritts and Luo, 1993). In the planetary boundary layer, the observed effects of a solar eclipse include the modulation of surface fluxes and a reduction in turbulence intensities. The influence of the eclipse shadow on the surface energy budget has been analysed in various climate zones, but so far never in the Arctic. Micrometeorological measurements during total solar eclipse events in the mid-latitudes revealed a decrease of the turbulent fluxes with reduced values of turbulent kinetic energy caused by the eclipse shadow (Foken et al. 2001; Founda et al., 2009). An effect on the vertical temperature structure towards boundary layer stability was found during a total solar eclipse in the tropical convective zone (Rao et al., 2013). Likewise, a transformation in the stability of the near-surface air during an eclipse event producing atmospheric conditions similar to the initiation of a nocturnal inversion was observed in a desert zone (Eaton et al., 1997). Due to the sparseness of observational sites in high Northern latitudes, no Arctic observations of radiation and micro-meteorology in eclipse conditions exist so far.

Here, we present the complete set of surface radiation components and meteorological mast observations with 1 minute time resolution during the total solar eclipse event over Ny-Ålesund on 20 March 2015. This high resolution eclipse data set is intended as baseline for e.g. further micrometeorological studies analysing the sensitivity of the surface energy balance on abrupt changes of the surface radiation budget. Moreover, a solar eclipse is an excellent means to test radiative transfer models (Emde and Mayer, 2007). The Ny-Ålesund solar eclipse data set is available at the PANGAEA data repository under doi:10.1594/PANGAEA.854326.

2 Radiative and Meteorological Conditions on 20 March 2015

As Ny-Ålesund is located at 78.9°N, the site is affected by polar day and polar night conditions from 18 April to 24 August and from 24 October to 18 February, respectively. On 20 March, the diurnal cycle is characterized by regular day and night time conditions, with the sun about 12 hours above the horizon (Figure 1). Yet, as Ny-Ålesund is situated on the coastline with mountains to the South, the complex horizontal line (doi: 10.1594/PANGAEA.669522) prevents direct sun visibility for some parts of the day. The solar eclipse though occurred when the sun was above the mountains, allowing observations of the partial and total solar eclipse phases.

On 20 March 2015, solar observations in Ny-Ålesund were undisturbed in terms of cloudiness. The cloud base height measured by remote sensing with a Vaisala LD-40 ceilometer (http://doi.pangaea.de/10.1594/PANGAEA.854377) is shown in Figure 2a. Clearly, the earlier morning cloud cover on 20 March 2015 had vanished before daylight and in advance to the beginning of the solar eclipse, allowing perfect clear sky observation conditions. Only at about 23 UTC low clouds were again observed above the station. In fact, the synoptic situation on 20 March 2015 was very stable under the influence of a high pressure system centred over the Greenland Sea. The station level pressure was changing only marginal, with a maximum of 1024.7 hPa at about 10:40 UTC slowly decreasing by about 3 hPa within the next 12 hours. Without synoptic drag on the lower atmospheric wind field, the local conditions dominated the surface near wind. Throughout the clear sky phase of the day, the wind speed has been very low below about 3 m/s (Figure 2c). In the Ny Ålesund surroundings, these

Earth Syst. Sci. Data Discuss., doi:10.5194/essd-2016-2, 2016
Manuscript under review for journal Earth Syst. Sci. Data
Published: 25 January 2016

are favourable conditions for prevailing katabatic winds from the glaciers (Jocher et al., 2012). In these cases, the common south-east oriented surface near atmospheric flow along the fjord axis (Beine et al., 2001; Maturilli et al., 2013) is predominated by south-westerly winds from the mountains and glaciers South of Ny-Ålesund, bringing cold air to the station. On 20 March 2015, such cold air outflow events are reflected in the surface air temperature (Figure 2e). Being about 2 K higher in the presence of clouds in the early morning hours, the baseline temperature is rather stable around -18 to -17 °C during the rest of the day. Yet, short peaks of lower temperatures are observed. These are correlated with according changes in wind direction (Figure 2d), pointing to cold air advection to the station when the wind arrives from south-west, the direction of the Brøggerbreen glacier. Overall, the meteorological conditions for the observation of the total solar eclipse on 20 March 2015 in Ny-Ålesund were excellent. The detailed surface radiation measurements during the eclipse are described in the next section.

3 Surface Radiation Measurements during the Solar Eclipse

In Ny-Ålesund, the solar eclipse on 20 March 2015 started at 09:10 UTC and lasted until 11:11 UTC, with the total eclipse phase between 10:09:53 and 10:12:11 UTC. The event has been followed by instrumentation and by eye, and its spectacular view is shown in Figure 3.

The measured diurnal cycle of global radiation for 20 March 2015 is shown in Figure 4. Though clouds were not present during the sunlit part of the day, broad reduction in global radiation is observed while the sun is shaded by the mountains as illustrated in Figure 1. During the total phase of the solar eclipse the global radiation vanishes completely, generating a unique signal in the measured downward radiation.

The downward components of shortwave and the upward longwave radiation during the eclipse phase are shown in Figure 5. One quality control factor of BSRN sites is the availability of independent measurements of direct and diffuse radiation in addition to the global radiation. In Ny-Ålesund, the direct radiation is measured by a Kipp&Zonen CHP1 pyrheliometer on a Schulz&Partner solar tracker shared with the diffuse radiation measurement by a ball-shaded Kipp&Zonen CMP22. Global and reflected radiation are also detected by CMP22 instruments, while upward and downward longwave radiation are obtained by Eppley's PIR pyrgeometers (Maturilli et al., 2015).

The direct radiation normalized to the horizontal plane, the diffuse radiation and the global radiation are shown in the upper panel of Figure 5. The eclipse event emerges symmetrically in the shortwave radiation components, following the solar disk shading by the moon. The largest contribution to the global radiation is given by the direct radiation component, constituting about two thirds of the incoming solar radiation. The contribution by the diffuse radiation is on the one hand limited by the mountain surroundings as indicated by the horizontal line in Figure 1. On the other hand, the mountains are snow covered and thus contribute to the incoming diffuse radiation by reflection.

On 20 March 2015, also the ground underneath the radiation instrumentation set-up was snow covered, with a snow layer of about 30 cm height as measured by a Jenoptik snow depth sensor SHM30. As low solar elevation angles limit the reliability

Earth Syst. Sci. Data Discuss., doi:10.5194/essd-2016-2, 2016
Manuscript under review for journal Earth Syst. Sci. Data
Published: 25 January 2016

of the albedo retrieval, the albedo value SW_{up}/SW_{down}, = 0.7 found for the highest solar elevation on 20 March 2015 remains subject to high uncertainty. The resulting emitted upward longwave radiation is shown in the lower panel of Figure 5. As the emission of thermal radiation is temperature dependent, the course of the upward longwave radiation during the solar eclipse is not symmetrical. With the progression of the solar eclipse and the consequent reduction in downward solar radiation, the thermal cooling of the snow surface overwhelms. As a consequence, a tardily decrease in upward longwave radiation related to surface and / or surface near cooling was observed. As the longwave radiation measurements are temperature corrected with three internal temperature sensors, the decrease in upward longwave radiation is not caused by changes in air temperature. Instead, a decrease in the 2 meter temperature is observed with about 10 minutes delay to the decreasing LW_{up}. This cooling though is potentially related to the advection of colder air from the glacier since it occurs simultaneous to a change in wind direction (see Figure 2d). As periods with prevailing katabatic winds from the glaciers were observed throughout the day, the changing wind and air temperature conditions cannot unambiguously be attributed to the solar eclipse. With the returning sunlight after the total eclipse phase, also the upward longwave radiation gently inclines to reach its original level.

Close to the total eclipse phase, more measurement details of the shortwave radiation components become apparent (Figure 6). It turns out that the independent global radiation measurement falls to 0 Wm^{-2} in minutes 10:09 to 10:12 UTC, thus shortly before and shortly after the actual totality when considering minute mean values. In fact, for the small irradiance values during the eclipse, the accuracy of the instruments needs to be taken into account. For the CMP22 used for the global radiation measurement, the zero offset type A due to the inner dome having a different temperature from the cold junctions of the sensor is given with < 3 Wm^{-2} by the manufacturer, as well as a directional response < 5 Wm^{-2}. These effects may also affect the measurement of diffuse radiation with a similar CMP22. The values for the diffuse radiation drop to 0 Wm^{-2} even earlier and then rise later, probably also related to the fact that the pyranometer for the detection of diffuse radiation is shaded by a ball slightly larger than the sun disk, thus covering a small fraction of the sky that is still visible for the global radiation measurement. The signal of direct solar radiation detected by pyrheliometer vanishes for the shortest period.

4 Atmospheric Profiles

Three Vaisala RS92 radiosondes have been launched from Ny-Ålesund during the eclipse period on 20 March 2015, at 08:39 UTC, at 10:10 UTC, and at 11:14 UTC. The Ny-Ålesund radiosonde program is certified by the Glocal Climate Observing Systems (GCOS) Reference Upper-Air Network (GRUAN), providing radiosonde data in reference quality. The radiosonde launched at 11:14 UTC has therefor been processed by GRUAN, and is available with quantitative uncertainty values for every measurement point.

The temperature profiles in the lowermost 300 metres of the atmosphere are shown in Figure 7. As the balloons have a rise rate of 5 m/s, the vertical profiles should be considered snap-shots of the atmospheric state. In all profiles, a surface based inversion below 100 metres altitude indicates stable conditions in the planetary boundary layer. Above the inversion, the

Earth Syst. Sci. Data Discuss., doi:10.5194/essd-2016-2, 2016
Manuscript under review for journal Earth Syst. Sci. Data
Published: 25 January 2016

temperature decreases following more or less the adiabatic temperature gradient, slightly differing from one profile to the next. Considering the measurement accuracy and the temperature uncertainty shown for the GRUAN processed profile (Figure 7), potential changes in the altitude of the surface based inversion top fall within the detection limit of the instrumentation. Overall, no temperature changes in the vertical column can be attributed to the solar eclipse. Before, during, and after the eclipse, the boundary layer was characterized by very stable conditions.

5 Summary

Adding to the long-term surface radiation observations from Ny-Ålesund (Maturilli et al., 2015), the rare event of a total solar eclipse has been measured by BSRN instrumentation on 20 March 2015. Under favourable meteorological conditions, the eclipse left its imprint on the surface radiation diurnal cycle. The according dataset (doi: 10.1594/PANGAEA.854326) provides highest quality measurement data of direct, diffuse, global and shortwave reflected radiation, upward and downward longwave radiation, as well as 2-meter temperature, relative humidity and station-level pressure in 1-minute resolution. Embedded in the larger frame of long-term surface radiation monitoring data, the solar eclipse data presented here provide the unique occasion to study the atmospheric response to rapid cut-off and turn-on of solar radiation under low solar elevation angles in an Arctic environment. In a larger frame, the data may provide potential benefit to radiative transfer model evaluation or satellite data validation. On a more local scale, the eclipse radiation data complement in–situ and remote sensing experiments operated in Ny-Ålesund. As one of the main concerns of current Arctic research is the energy budget at the Earth's surface, the presented surface radiation measurements contribute as a baseline to the various Ny-Ålesund boundary layer studies, including turbulent flux measurements of sensible and latent energy. The surface radiation data may also support the discussion of e.g. a photochemical response in measured atmospheric trace gases, or radiation and temperature related changes in the fjord's sea surface layer. Overall, the research multiplicity of the Arctic research centre Ny-Ålesund offers various possibilities to apply the solar eclipse radiation data for process studies under free atmospheric laboratory conditions switched to abrupt night time conditions.

Acknowledgements: The authors thank the station personnel of the AWIPEV research base in Ny-Ålesund for maintaining the instrumentation and operating the measurements. Particular thanks to S. Debatin for data validation. We thank Nathalie Grenzhaeuser for providing the photo (Figure 3).

Earth Syst. Sci. Data Discuss., doi:10.5194/essd-2016-2, 2016
Manuscript under review for journal Earth Syst. Sci. Data
Published: 25 January 2016

Open Access Earth System Science Data Discussions

References:

Anderson, R. C., and Keefer D. R.: Observation of temperature and pressure changes during 30 June 1973 solar eclipse, J. Atmos. Sci., 32, 228–231, 1975.

Anderson, R. C., Keefer, D. R., and Myers, O. E.: Atmospheric-pressure and temperature changes during 7 March 1970 solar eclipse, J. Atmos. Sci., 29, 583–587, 1972.

Beine, H. J., Argentini, S., Maurizi, A., Mastrantonio, G., and Viola, A.: The local wind field at Ny-Ålesund and the Zeppelin mountain at Svalbard, Meteorol. Atmos. Phys., 78, 107-113, doi: 10.1007/s007030170009, 2001.

Eaton, F. D., Hines, J. R., Hatch, W. H., Cionco, R. M., Byers, J., Garvey, D., and Miller, D. R.: Solar eclipse effects observed in the planetary boundary layer over a desert, Bound.-Layer Meteor., 83, 331–346, 1997.

Emde, C., and Mayer, B.: Simulation of solar radiation during a total eclipse: a challenge for radiative transfer, Atmos. Chem. Phys., 7, 2259-2270, doi:10.5194/acp-7-2259-2007, 2007.

Fritts, D. C., Luo, Z. G.: Gravity-wave forcing in the middle atmosphere due to reduced ozone heating during a solar eclipse, J. Geophys. Res., 98, 3011–3021, doi:10.1029/92JD02391, 1993.

Foken, T., Wichura, B., Klemm, O., Gerchau, J., Winterhalter, M., and Weidinger, T.: Micormeteorological measurements during the total solar eclipse of August 11, 1999, Meteorol. Zeitschrift, 10, 171-178, doi: 10.1127/0941-2948/2001/0010-0171, 2001

Founda, D., Lykoudis, S., Psiloglou, B. E., Petrakis, M., and Zerefos, C.: Observations of the atmospheric surface layer parameters during the total solar eclipse of March 29th, in Greece, Meteorol. Zeitschrift, 18, 489-494, doi: 10.1127/0941-2948/2009/0406, 2009.

Goodwin, G. L., and Hobson, G. J.: Atmospheric gravity waves generated during a solar eclipse, Nature, 275, 109-111, doi:10.1038/275109a0, 1978.

Jocher, G., Karner, F., Ritter, C., Neuber, R., Dethloff, K., Oberleitner, F., Reuder, J., and Foken, T.: The near-surface small-scale spatial and temporal variability of sensible and latent heat exchange in the Svalbard region: a case study, ISRN Meteorology, Vol. 2012, Article ID 357925, doi: 10.5402/2012/357925, 2012.

Marty, J., Dalaudier, F., Ponceau, D., Blanc, E., and Munkhuu, U.: Surface Pressure Fluctuations Produced by the Total Solar Eclipse of 1 August 2008, J. Atmos. Sci., 70, 809-823, doi: 10.1175/JAS-D-12-091.1, 2013.

Maturilli, M., Herber, A., and König-Langlo, G.: Climatology and time series of surface meteorology in Ny-Ålesund, Svalbard, Earth Syst. Sci. Data, 5, 155–163, doi: 10.5194/essd-5-155-2013, 2013.

Maturilli, M., Herber, A., and König-Langlo, G.: Surface radiation climatology for Ny-Ålesund, Svalbard (78.9°N), basic observations for trend detection, Theor. Appl. Climatol., 120, 331-339, doi: 10.1007/s00704-014-1173-4, 2015.

Rao, K. G., Reddy. N. N., Ramakrishna, G., Bhuyan, P. K., Bhuyan, K., Kalita, G., and Pathak, B.: Near surface atmospheric response to the total solar eclipse at Dibrugarh on 22 July 2009, J. Atmos. Sol.-Terr. Phy., 95-96, 87-95. doi: 10.1016/j.jastp.2013.01.001, 2013.

Earth Syst. Sci. Data Discuss., doi:10.5194/essd-2016-2, 2016
Manuscript under review for journal Earth Syst. Sci. Data
Published: 25 January 2016

Schödel, J. P., Klostermeyer, J., and Röttger, J.: Atmospheric Gravity Wave Observations after the Solar Eclipse of June 30, 1973, Nature, 245, 87-88, doi:10.1038/245087a0, 1973.

Seykora, E. J., Bhatnagar, A., Jain, R. M., and Streete, J. L.: Evidence of atmospheric gravity waves produced during the 11 June 1983 total solar eclipse, Nature, 313, 124-125, doi: 10.1038/313124a0, 1985.

Earth Syst. Sci. Data Discuss., doi:10.5194/essd-2016-2, 2016
Manuscript under review for journal Earth Syst. Sci. Data
Published: 25 January 2016

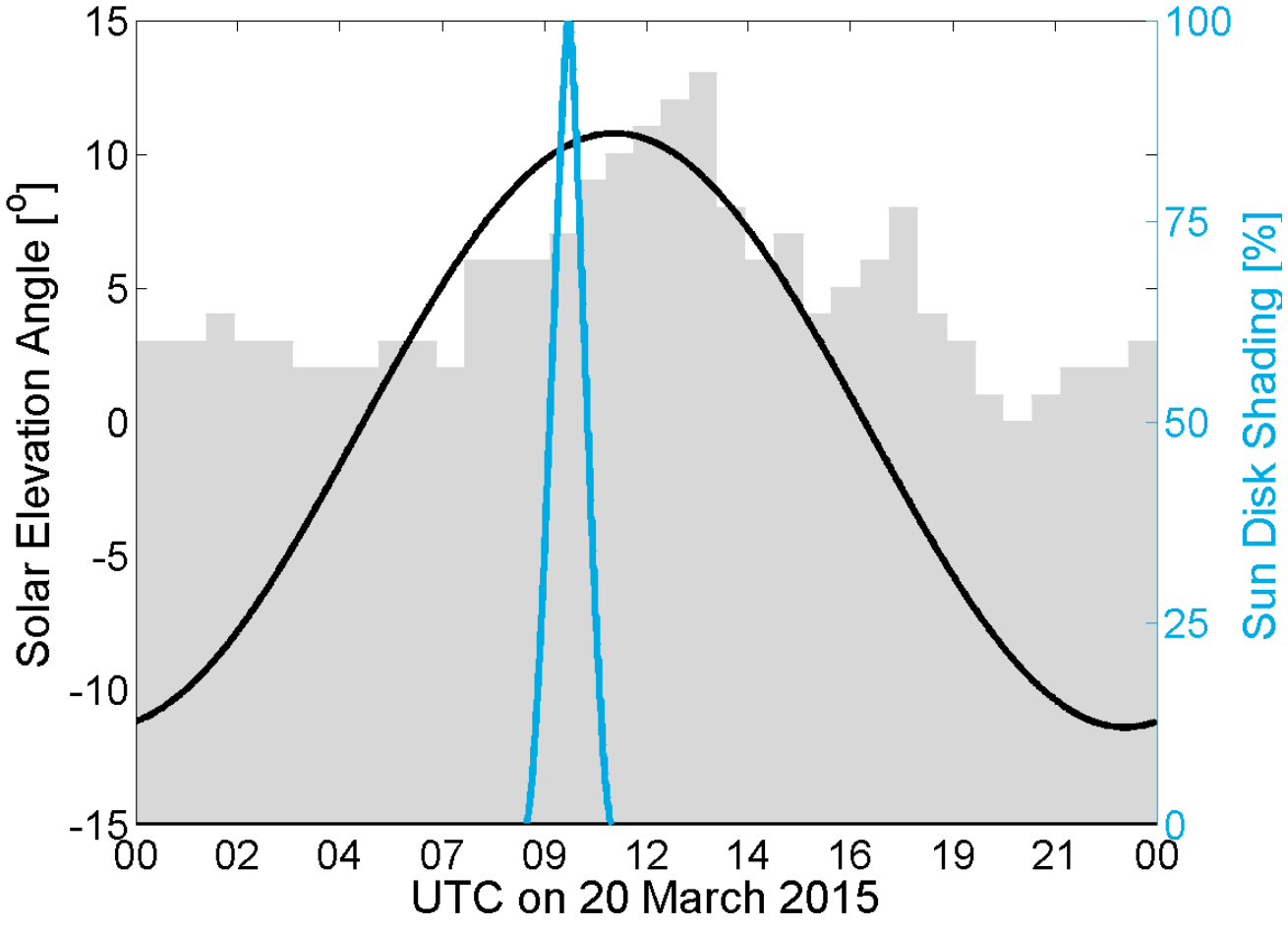

Fig. 1: Solar elevation angle (black line) for Ny-Ålesund coordinates (78.9° N, 11.9° E) on 20 March 2015, with local horizontal line (grey shading), respectively. The totality of the solar eclipse is indicated (cyan line).

Earth Syst. Sci. Data Discuss., doi:10.5194/essd-2016-2, 2016
Manuscript under review for journal Earth Syst. Sci. Data
Published: 25 January 2016

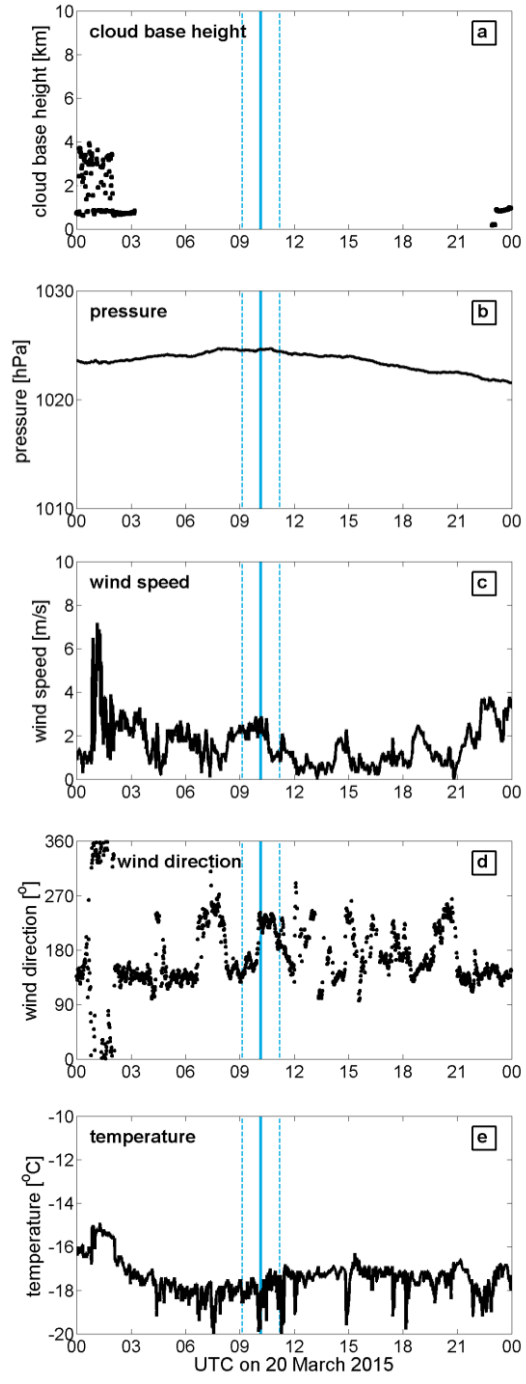

Fig. 2: Meteorological surface observations in Ny-Ålesund on 20 March 2015, with (a) cloud base height,(b) station level pressure, (c) 10 meter wind speed, (d) 10 meter wind direction, and (e) surface air temperature at 2 m height. Indicated is the duration of the solar eclipse (dashed blue lines, respectively) and the time of total eclipse (blue line).

Earth Syst. Sci. Data Discuss., doi:10.5194/essd-2016-2, 2016
Manuscript under review for journal Earth Syst. Sci. Data
Published: 25 January 2016

Fig. 3: Solar eclipse over Ny-Ålesund, Svalbard. (Photo: Nathalie Grenzhaeuser)

Earth Syst. Sci. Data Discuss., doi:10.5194/essd-2016-2, 2016
Manuscript under review for journal Earth Syst. Sci. Data
Published: 25 January 2016

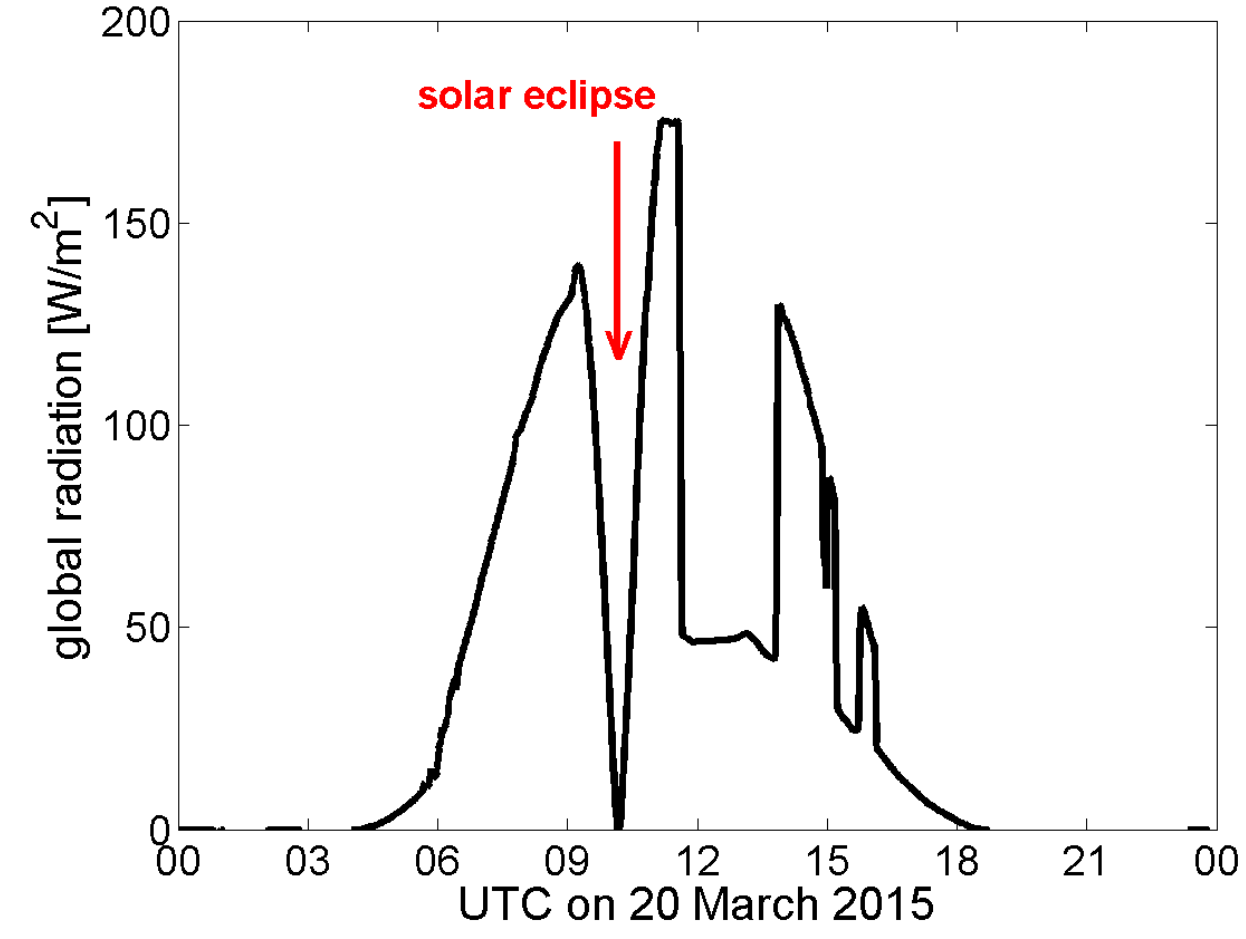

Fig. 4: Ny-Ålesund global radiation (SWdown) on 20 March 2015, measured by a Kipp&Zonen pyranometer CMP22. After 12 UTC, the deviation from the sinusoidal curve is related to shading by mountains.

Earth Syst. Sci. Data Discuss., doi:10.5194/essd-2016-2, 2016
Manuscript under review for journal Earth Syst. Sci. Data
Published: 25 January 2016

Open Access Earth System Science Data Discussions

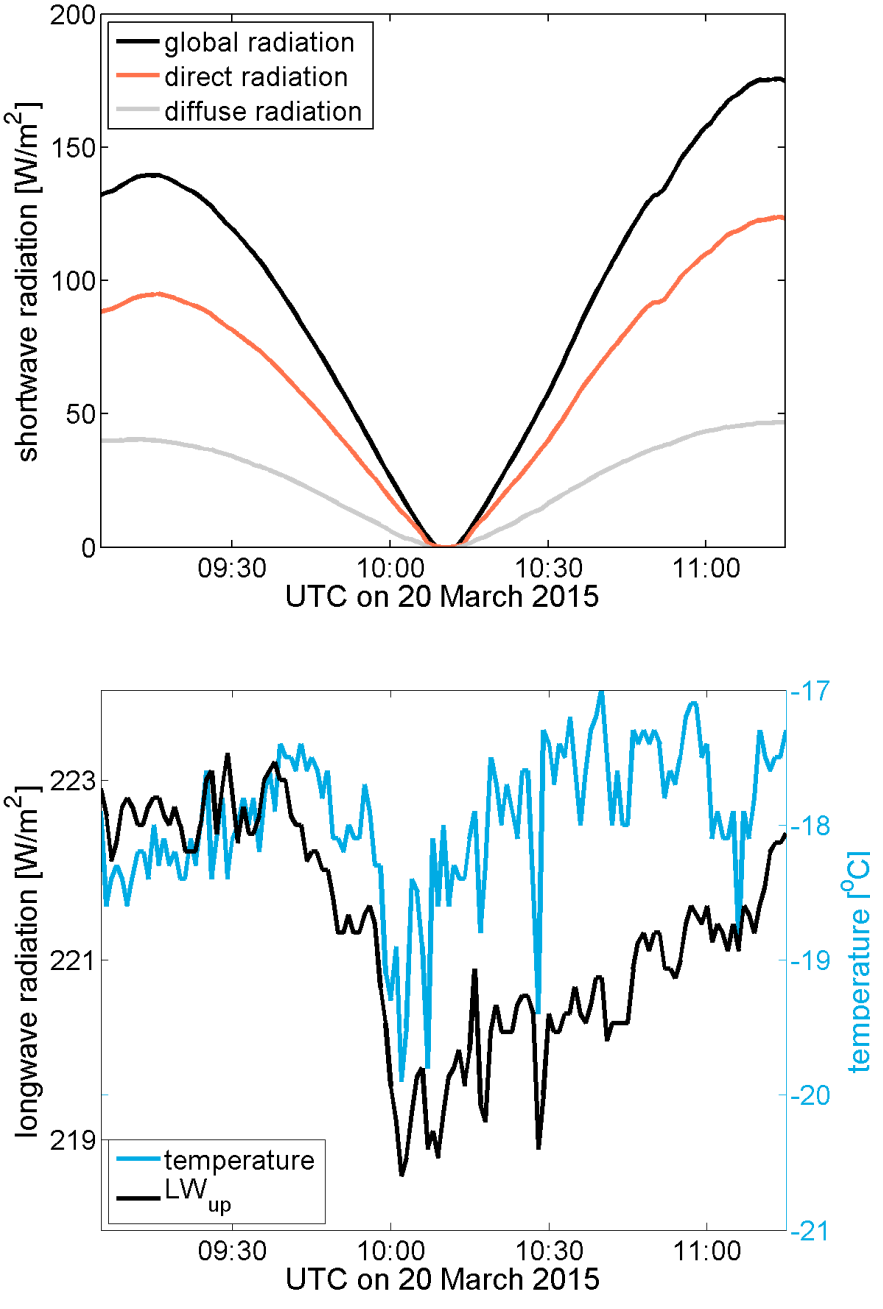

Fig. 5: The downward shortwave radiation components direct, diffuse and global radiation (upper panel) as well as the upward thermal radiation LWup and 2-meter temperature (lower panel) between 9:10 and 11:10 UTC on 23 March 2015 in Ny-Ålesund

Earth Syst. Sci. Data Discuss., doi:10.5194/essd-2016-2, 2016
Manuscript under review for journal Earth Syst. Sci. Data
Published: 25 January 2016

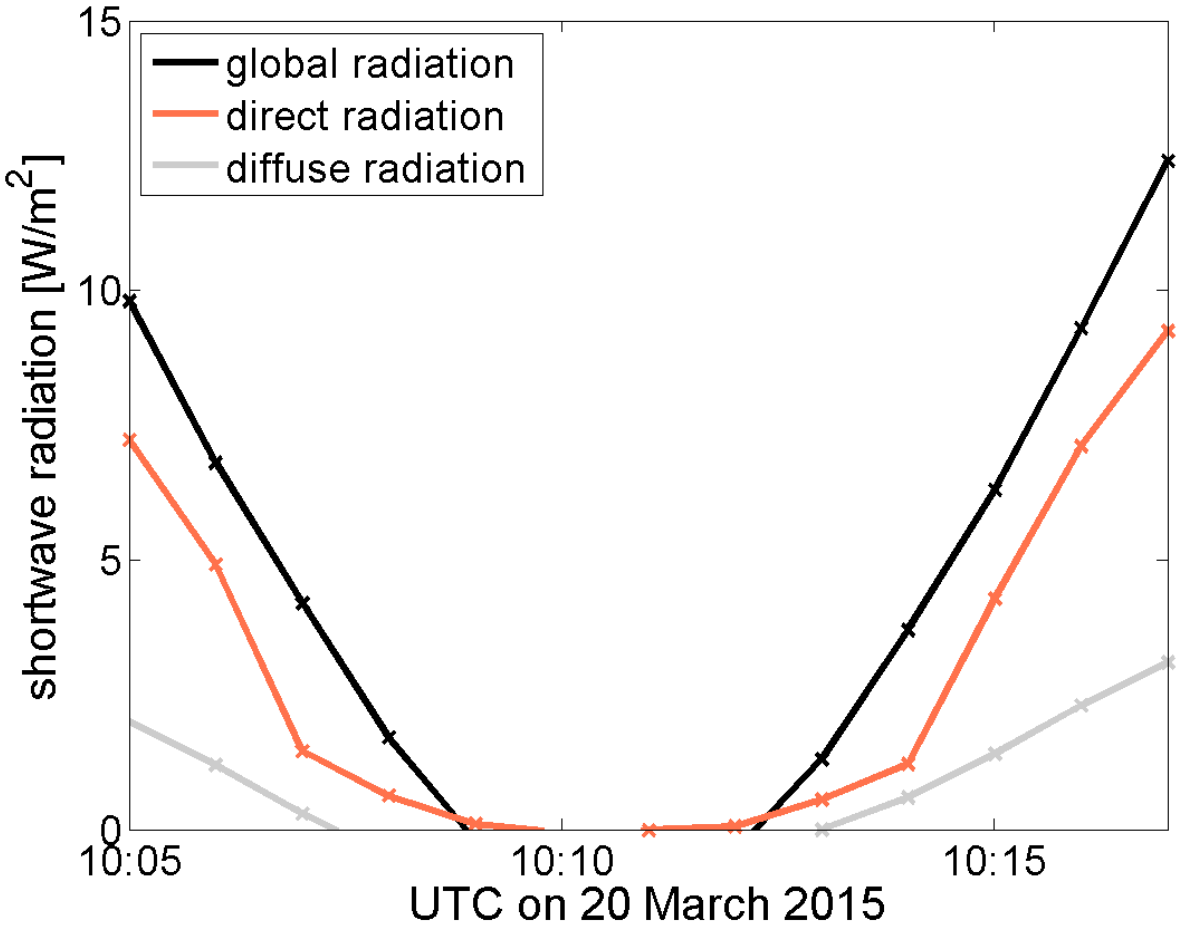

Fig. 6: The downward shortwave radiation components direct, diffuse and global radiation during the total eclipse phase.

Earth Syst. Sci. Data Discuss., doi:10.5194/essd-2016-2, 2016
Manuscript under review for journal Earth Syst. Sci. Data
Published: 25 January 2016

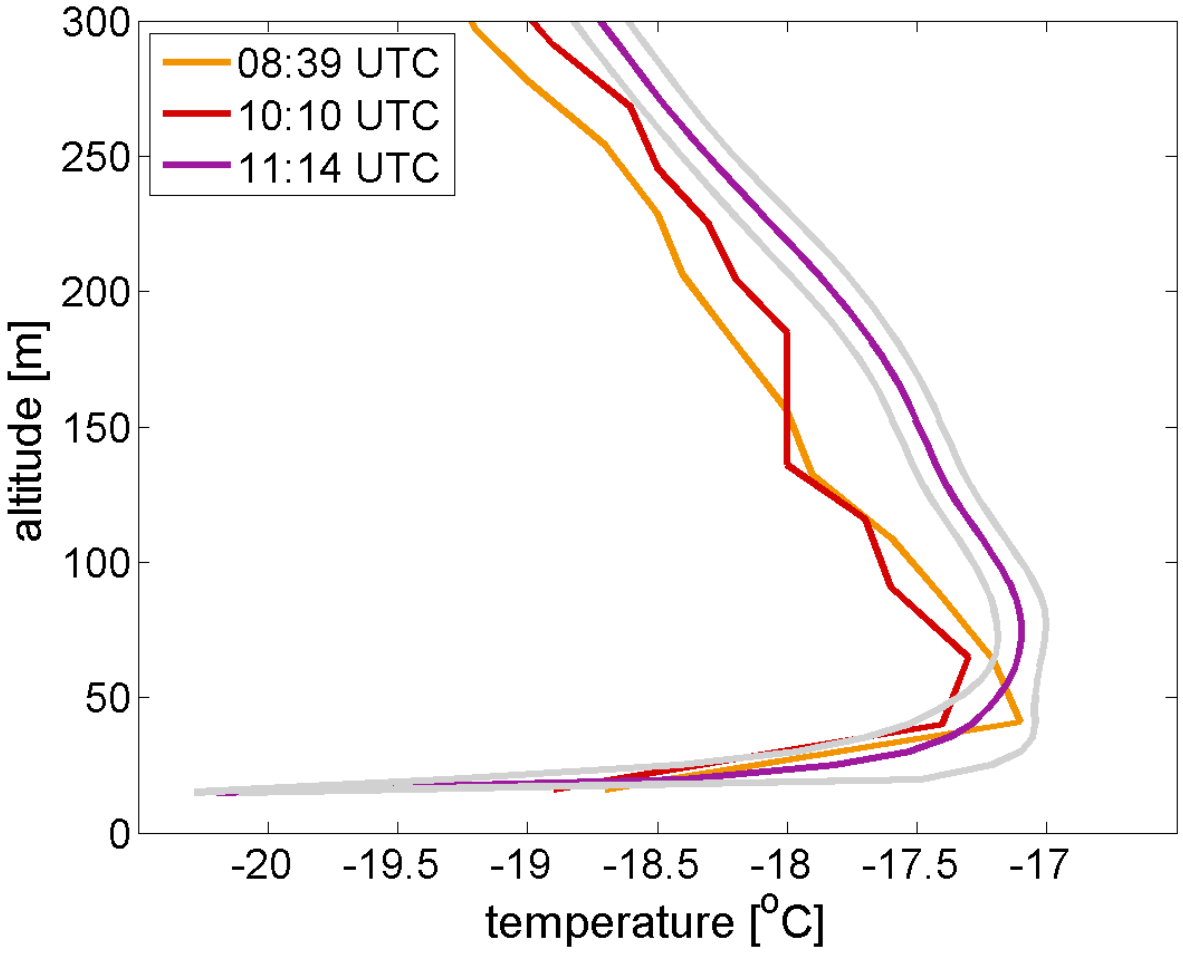

Fig. 7: Vertical temperature profiles measured by RS92 radiosondes launched from Ny-Alesund on 20 March 2015. The radiosonde launched at 11:14 UTC has been processed as GRUAN reference sonde, and the according temperature profile (purple line) is provided with measurement uncertainty in each altitude level (grey lines).